



ELSEVIER

Journal of Alloys and Compounds 234 (1996) 43–47

Journal of  
ALLOYS  
AND COMPOUNDS

# Mechanical alloying of Fe and Zn: phase analysis and Mössbauer studies

J.C. de Lima<sup>a</sup>, E.C. Borba<sup>a</sup>, C. Paduani<sup>a</sup>, V.H.F. dos Santos<sup>a</sup>, T.A. Grandi<sup>a</sup>,  
H.R. Rechenberg<sup>b</sup>, I. Denicoló<sup>c</sup>, M. Elmassalami<sup>d</sup>, A.F. Barbosa<sup>d</sup>

<sup>a</sup>Departamento de Física, Universidade Federal de Santa Catarina, Florianópolis CEP 88040-900, Santa Catarina, Brazil

<sup>b</sup>Instituto de Física, Universidade de São Paulo, São Paulo, Brazil

<sup>c</sup>Departamento de Física, Universidade Federal do Paraná, Curitiba, Brazil

<sup>d</sup>Centro Brasileiro de Pesquisas Físicas, Rio de Janeiro, Brazil

Received 18 October 1994; in final form 19 September 1995

## Abstract

Crystalline Fe<sub>25</sub>Zn<sub>75</sub> powder alloys ( $\Gamma_1$  phase) have been prepared by mechanical alloying of pure elemental powders. A crystalline Fe<sub>27.9</sub>Zn<sub>72.1</sub> alloy ( $\Gamma$  phase) was obtained after adequate annealing. The Mössbauer spectra at room temperature displayed three doublets before annealing, corresponding to iron atoms located at the outer tetrahedral, inner tetrahedral and octahedral sites in the unit cell of Fe<sub>25</sub>Zn<sub>75</sub>. For the annealed sample, two doublets associated with iron atoms located at two tetrahedral inequivalent sites in the unit cell of Fe<sub>27.9</sub>Zn<sub>72.1</sub> were observed. This  $\Gamma_1$ -to- $\Gamma$ -phase transition was confirmed by X-ray diffraction and Mössbauer spectroscopy measurements.

**Keywords:** Mechanical alloying; Fe; Zn; Phase analysis; Mössbauer spectroscopy

## 1. Introduction

Fe–Zn alloys have a great industrial importance, particularly in automotive industries, where they are applied as anticorrosive coating material for steel sheets. The quality of coating depends on the distribution of zinc within the coating layer. On the contrary, the large difference between the melting points of the elemental zinc (420 °C) and iron (1535 °C) makes it difficult to obtain Fe–Zn alloys at specific compositions by conventional techniques.

It is well known that mechanical alloying (MA) is a dry milling process in which a metallic and/or non-metallic powder mixture is actively deformed in a controlled atmosphere, under a highly energetic ball charge to produce a composite metallic powder. The few thermodynamics restrictions on the alloy composition open up a wide range of possibilities for property combinations [1], even for immiscible elements [2]. The temperatures reached in MA are very low, and thus this low temperature process reduces reaction kinetics, allowing the production of poorly crystallized or amorphous materials [1]. This indicates that the

difficulty of preparing binary alloys when the constituents have large melting points differences, such as zinc and iron, can be overcome using the MA technique. However, for poorly crystallized materials produced by MA several difficulties arise: (i) the final product contains lattice defects and strains, and thus a heat treatment becomes necessary to promote structural relaxation and; (ii) the mean size of the crystallites reached in MA is very small (nanometer size), a fact that complicates the interpretation of the X-ray diffraction (XRD) pattern due to the enlargement produced in the peaks.

Initially, the Fe–Zn phase diagram showed an extensive  $\alpha$ -Fe solubility area, a closed  $\gamma$  loop and three compounds in the Zn-rich region denoted  $\Gamma$ ,  $\delta$  and  $\zeta$  phases [3]. Later, a new compound, called  $\Gamma_1$ , containing 76.5–81.5 at.% Zn was found by Bastin et al. [4]. It has an f.c.c. cell with a cell parameter  $a = 17.963 \text{ \AA}$  and space group  $F\bar{4}3m$ . The Fe<sub>22</sub>Zn<sub>78</sub> compound was investigated by Koster and Schoone [5], confirming the results found by Bastin et al. According to [3], the  $\Gamma$  phase is isotypic with a  $\gamma$  brass structure and it has a b.c.c. cell with a cell parameter

varying linearly from  $a = 8.974 \text{ \AA}$  at 68.7 at.% Zn up to  $a = 9.018 \text{ \AA}$  at 76.3 at.% Zn. New refinements of the  $\gamma$ -brass-type structures  $\text{Cu}_5\text{Zn}_8$ ,  $\text{Cu}_5\text{Cd}_8$  and  $\text{Fe}_3\text{Zn}_{10}$  have been carried out by Brandon et al. [6]. Besides the determination of the space group ( $I\bar{4}3m$ ) for these three compounds, these workers have produced refined data for the atomic coordinates and for the thermal parameters.

Recently, the  $\Gamma$ ,  $\Gamma_1$ ,  $\delta$  and  $\zeta$  phases were studied with Mössbauer spectroscopy (MS) at room temperature (RT) and XRD by Gu et al. [7]. All alloys studied in [7] were prepared in two steps because of the difficulty of preparing Fe–Zn alloys.

In this work, we show that the  $\Gamma_1$  phase of the  $\text{Fe}_{25}\text{Zn}_{75}$  compound can be produced at RT in a simple fashion by milling pure elemental powders of iron and zinc. A crystallographic phase transition to  $\Gamma$  phase was obtained after an appropriate annealing. The experimental techniques of XRD, MS and differential scanning calorimetry (DSC) were used to investigate both the structural and the magnetic properties of these two alloys.

## 2. Experimental procedures

High purity elemental powders of iron (purity, 99.99%) and zinc (purity, 99.98%) were mixed in the nominal composition of  $\text{Fe}_{25}\text{Zn}_{75}$ . Together with this mixture, we put ten steel balls (nine balls of 10 mm diameter and one of 20 mm diameter) sealed into a cylindrical steel vial under argon atmosphere. The weight ratio of the balls to powder was 5 to 1. A planetary ball mill was then used to perform MA at RT. At selected times, we stop milling to obtain small amounts of samples for analysis by opening the vial within a glove-box. In order to determine the possible  $\Gamma_1$ -to- $\Gamma$  phase transition temperature, a small amount (about 8.90 mg) of each sample was used to carry out DSC measurements from  $30^\circ\text{C}$  up to  $600^\circ\text{C}$  at a rate of  $10^\circ\text{C min}^{-1}$ . After that, all samples were sealed in a quartz tube evacuated at about  $10^{-5}$  Torr and annealed at  $250^\circ\text{C}$  for 24 h, followed by air cooling. The XRD patterns were collected using  $\text{Cu K}\alpha$  radiation ( $\lambda = 1.5418 \text{ \AA}$ ). The Mössbauer spectra were also collected at RT in the transmission geometry with a  $^{57}\text{Co}$ –Rh source with a conventional spectrometer. The DSC spectra were measured with a Shimadzu DSC BSC-50 model.

## 3. Results and discussion

Small amounts of reacted powder were collected after milling for 170, 360, 400 and 854. The milled samples consist of a black powder, which had already

been observed after milling for 170 h. The XRD patterns obtained for all samples are identical, showing a stable phase quite different of that for pure elements. Fig. 1 shows the XRD patterns for the sample obtained after milling for 854 h (curve (a) shows the patterns for the sample and curve (b) for those after annealing). We can see that quite different patterns were measured before and after the annealing process.

It has been mentioned previously that MA is a low temperature process, which provides poorly crystallized or an amorphous materials. Therefore the XRD pattern or any other property from an as-milled material must be interpreted carefully, mainly when they are compared with those from crystals. Keeping this in mind, it can be seen that the analysis of the XRD pattern measured for the as-milled sample shown in Fig. 1, curve (a) is a difficult task. There are two main reasons for this: (i) the final product is not well crystallized and contains all types of lattice defect and strain and (ii) the mean size of the crystallites is very small, causing an enlargement of all peaks shown in the XRD pattern, making it difficult to distinguish the occurrence of other peaks when the peaks are located very close together. Despite these difficulties, indexing was attempted for this XRD pattern and is described later.

From the XRD patterns shown in Fig. 1, the mean size of the crystallites were estimated considering the higher peaks and the Scherrer formula  $L = 0.91\lambda / (\beta \cos \theta)$  [8], where  $\lambda$  is the X-ray wavelength,  $\beta$  is the width (full width at half-maximum) of the pure diffraction profile on the  $2\theta$  scale in radians. The values

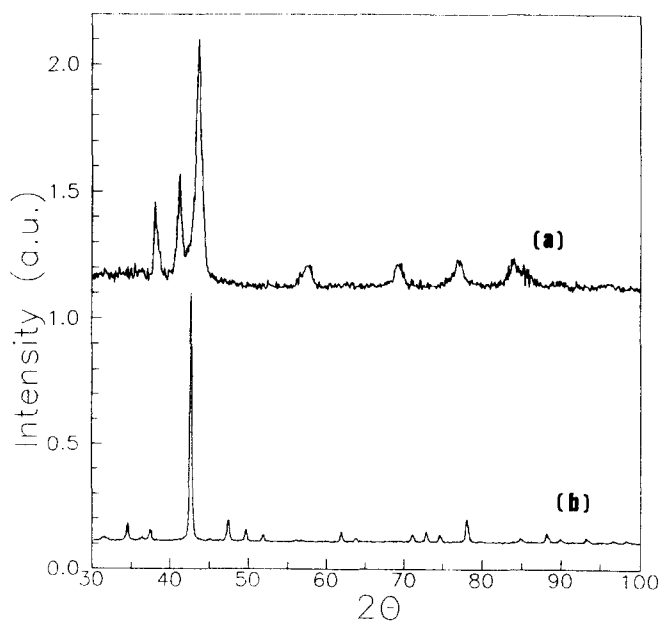


Fig. 1. XRD patterns (a.u., arbitrary units): curve (a), as-milled  $\text{Fe}_{25}\text{Zn}_{75}$ ; curve (b), after annealing,  $\text{Fe}_{27.9}\text{Zn}_{72.1}$ .

found are about  $L = 96 \text{ \AA}$  and  $L = 270 \text{ \AA}$  for the as-milled sample (Fig. 1, curve (a)) and for the sample after annealed (Fig. 1, curve (b)) respectively.

The nominal composition of the mixture that we chose is  $\text{Fe}_{25}\text{Zn}_{75}$ . Therefore we expected to obtain the  $\Gamma$  phase. Based on this assumption, we have tried to index the XRD pattern showed in Fig. 1, curve (a), to a b.c.c. cell, but the calculated pattern did not agree with the angular positions observed. The  $\delta$  and  $\zeta$  phases were also tried without success. Finally, we tried to index this pattern to the  $\Gamma_1$  phase. Considering the angular positions of the six main peaks, a least-squares fitting procedure indicates that the observed phase is f.c.c., with a cell parameter  $a = 18.0138 \text{ \AA}$ . The difference between this value and those from [4,5] can be associated with the difference between the compositions.

Furthermore, we used the data from [5] for the atomic coordinates, temperature factors and space group in a Rietveld structure refinement procedure to refine the XRD pattern shown in Fig. 1(a). The simulated XRD pattern exhibits several peaks located between  $45^\circ$  and  $55^\circ$  where in our data there are no peaks. On the contrary, by changing only the space group for  $F\bar{4}3c$  we observed that these peaks have disappeared. So, we kept this latter space group. In both cases, the XRD pattern measured was only reproduced partially, considering the presence of two independent compounds both having an f.c.c. cell with parameters  $a = 17.5638 \text{ \AA}$  and  $a = 18.6138 \text{ \AA}$ . The mean cell parameter obtained from the two compounds is  $a = 18.0888 \text{ \AA}$ , which agrees with the value of  $a = 18.0138 \text{ \AA}$ , calculated by the least-squares refinement procedure. Fig. 2, data A, shows the measured and simulated patterns and Fig. 2, curve B, their difference. From this figure it can be seen that the four peaks located at about  $38.7^\circ$ ,  $41.5^\circ$ ,  $43.8^\circ$  and  $77.2^\circ$  are reproduced, while those located at about  $58^\circ$ ,  $69.5^\circ$  and  $84^\circ$  are not. Probably there is another phase present, which was not possible to identify. Several workers [9] have reported the formation of two or more phases simultaneously through the MA technique. To our knowledge, this is the first time that the  $\Gamma_1$  phase is obtained by MA technique.

The DSC curves measured for all collected samples have similar shapes. Fig. 3 shows the DSC curve for the sample collected after milling for 854 h. This picture shows a strong exothermic peak at about  $197^\circ\text{C}$ . The corresponding energy is  $5.9 \text{ cal g}^{-1}$  which is associated with the  $\Gamma_1$ -to- $\Gamma$ -phase transition besides promoting structural relaxation by removing lattice defects and strains introduced by the MA process.

For the annealed sample, firstly we have indexed the XRD pattern shown in Fig. 1, curve (b), by a least-squares refinement procedure, considering the angular positions of all peaks measured for a b.c.c. cell with a

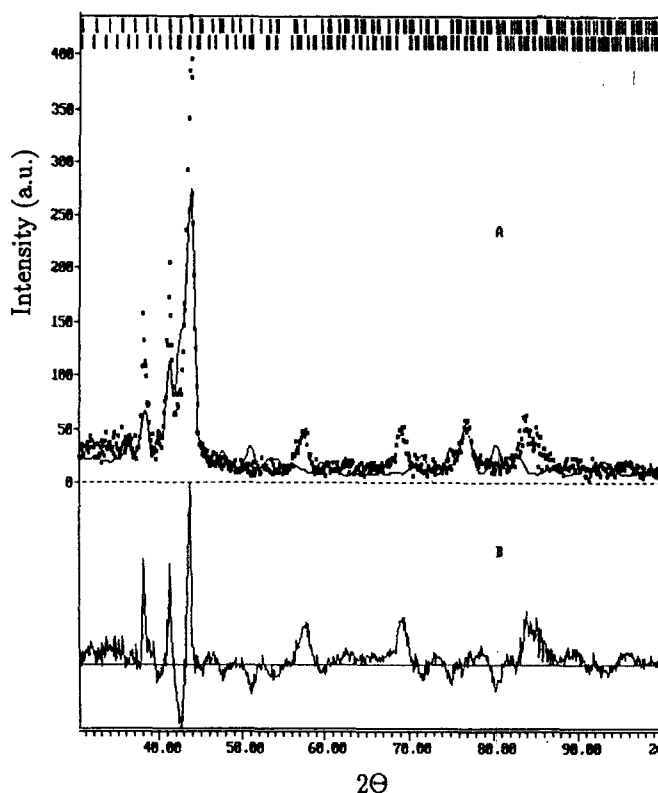


Fig. 2. XRD patterns (a.u., arbitrary units): data A, experimental (■) and calculated (—) for as-milled  $\text{Fe}_{25}\text{Zn}_{75}$ ; curve B, their difference.

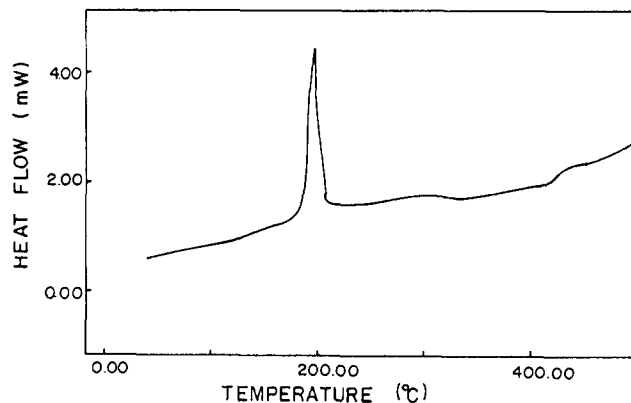


Fig. 3. DSC result for as-milled  $\text{Fe}_{25}\text{Zn}_{75}$ .

cell parameter  $a = 8.9936 \text{ \AA}$ . Then we considered the space group  $I\bar{4}3m$  and the refined data for the  $\text{Fe}_3\text{Zn}_{10}$  compound ( $\Gamma$  phase) given in [6], to simulate the measured XRD pattern using the Rietveld [10] structure refinement method. Fig. 4 shows the measured and simulated patterns for the annealed sample. From this picture, we can see excellent agreement between the measured and simulated patterns, confirming that the as-milled sample ( $\Gamma_1$  phase) undergoes a phase transition to a final product ( $\Gamma$  phase) after annealing as well as a grain growth process, as determined by the Scherrer formula. Following the linear dependence of the cell parameter on zinc concentration [3] for the  $\Gamma$

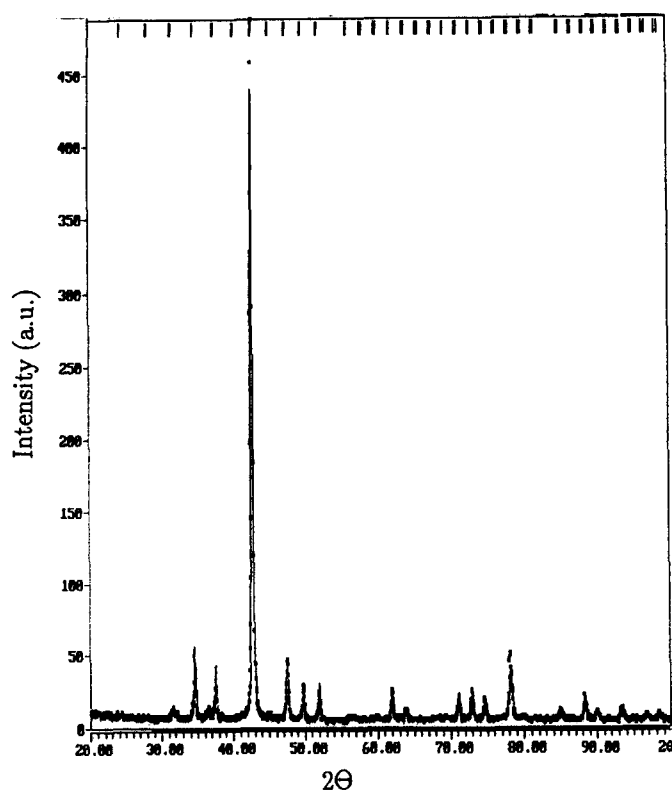


Fig. 4. Experimental (■) and calculated (—) XRD patterns for  $\text{Fe}_{27.9}\text{Zn}_{72.1}$  (a.u., arbitrary units).

phase, the value of  $a = 8.9936 \text{ \AA}$  corresponds to 72.1 at.% Zn, indicating a loss of zinc of about 2.9 at.% Zn caused by the heat treatment.

The Mössbauer spectra of the four as-milled samples have similar shapes. Figures 5 and 6 show the Mössbauer spectra measured for the sample collected after milling for 854 h, before and after annealing, respectively. By comparing the Figs. 5 and 6, large differences between these two Mössbauer spectra are evident. In order to understand the differences between the Mössbauer spectra, it is necessary to know the details of the crystalline structures for both the  $\Gamma_1$  and the  $\Gamma$  phases.

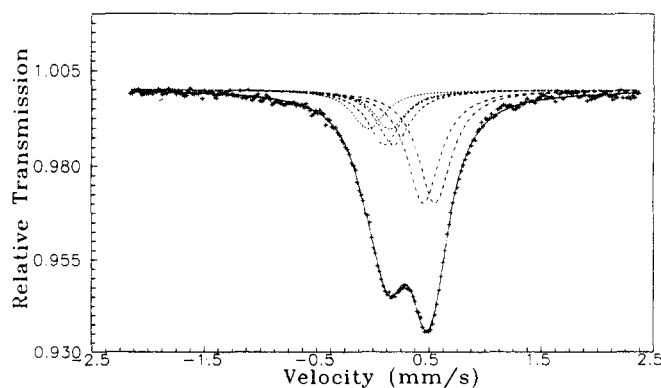


Fig. 5. Mössbauer spectrum at RT for as-milled  $\text{Fe}_{25}\text{Zn}_{75}$ ; —, fit; subspectra; + experimental data.

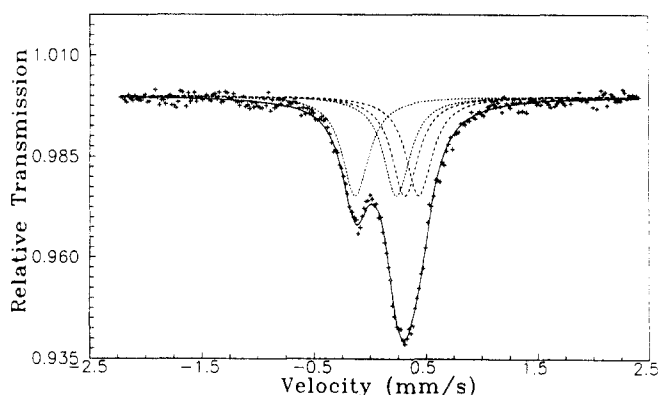


Fig. 6. Mössbauer spectrum at RT after annealing, i.e.  $\text{Fe}_{27.9}\text{Zn}_{72.1}$ ; —, fit; subspectra; +, experimental data.

For this compound several stoichiometric formulas have been reported [4,5,6,11]. Both  $\text{Fe}_3\text{Zn}_{10}$  and  $\text{Fe}_8\text{Zn}_{18}$  are  $\Gamma$  phases, with a cubic  $\gamma$ -brass structure with 52 atoms per unit cell. The 12 iron atoms in the unit cell of  $\text{Fe}_3\text{Zn}_{10}$  have two kinds of position, four in the inner tetrahedral (IT) sites and eight in the outer tetrahedral (OT) sites [6]. Moreover, of the 16 atoms in the unit cell of  $\text{Fe}_8\text{Zn}_{18}$ , eight are located in IT sites and eight in octahedral (OH) positions [11]. The  $\Gamma_1$  phase of  $\text{Fe}_{22}\text{Zn}_{78}$  is a cubic phase with 408 atoms per unit cell [5], in which, among the 90 iron atoms, 24 are in OH, 16 in OT, 16 in IT, and the remainder may be in the OT or IT positions [7]. The structure of the  $\Gamma_1$  phase was compared with that of the  $\Gamma$  phase obtained by Koster and Schoone [5] who pointed out that, if eight cells of  $\Gamma$  phase are stacked together, doubling the cell in the  $x$ ,  $y$  and  $z$  directions, a large cell with a space group of  $F\bar{4}3m$  is formed, and further that the natures of the atoms at the same position for the two crystal structures are not necessarily the same. These differences lead to different MS parameters for these two phases, as obtained in [7]. The nominal composition used in this study contains 25 at.% Fe, whose formulae can be given either as  $\text{Fe}_{25}\text{Zn}_{75}$  or  $\text{FeZn}_3$ . The detailed structure of this phase is unknown. Following the same procedure as [7] we fit the Mössbauer spectra measured for four as-milled samples ( $\Gamma_1$  phase) with three quadrupole doublets ( $\text{Fe}_1$ ,  $\text{Fe}_2$  and  $\text{Fe}_3$ ) corresponding to the quadrupole splitting arising from iron atoms in the three different sites. From the fitted parameters, the amplitude ratio of the three peaks is 2.9:1.4:1; so the number of iron atoms in the three positions in a unit cell can be roughly estimated as 56, 27 and 19 respectively.

The MS data points sets were fitted by the least-squares fitting method to standard Lorentzian curves. The Mössbauer parameters calculated from the fitting of the  $\Gamma_1$  phase are shown in Table 1. For comparison, we show in parentheses the results of Gu et al. [7] for the  $\text{FeZn}_4$  compound. The slight differences observed

Table 1

Mössbauer parameters for as-milled  $\text{Fe}_{25}\text{Zn}_{75}$  and after annealing, i.e.  $\text{Fe}_{27.9}\text{Zn}_{72.1}$  powders: isomer shift (IS), quadrupole splitting (QS) and line width  $\Gamma$ , where the values within parentheses are from [7]

Phase	Position	IS ( $\text{mm s}^{-1}$ )	QS ( $\text{mm s}^{-1}$ )	$\Gamma_{\text{exp}}$ ( $\text{mm s}^{-1}$ )
$\Gamma_1$	Fe <sub>1</sub>	0.502 ± 0.001 (0.442 ± 0.027)	0.102 ± 0.004 (0.091 ± 0.058)	0.353 (0.353 ± 0.014)
	Fe <sub>2</sub>	0.143 ± 0.023 (0.088 ± 0.151)	0.082 ± 0.055 (0.291 ± 0.072)	0.353 (0.353 ± 0.014)
	Fe <sub>3</sub>	0.055 ± 0.032 (−0.027 ± 0.095)	0.187 ± 0.058 (0.278 ± 0.101)	0.353 (0.353 ± 0.014)
$\Gamma$	Fe <sub>1</sub>	0.370 ± 0.001 (0.403 ± 0.002)	0.124 ± 0.005 (0.115 ± 0.006)	0.285 ± 0.003 (0.288 ± 0.008)
	Fe <sub>2</sub>	0.050 ± 0.002 (0.052 ± 0.005)	0.366 ± 0.003 (0.345 ± 0.008)	0.285 ± 0.003 (0.288 ± 0.008)

in the MS parameters are attributed to different compositions of the same phase (in this work containing 25 at.% Fe and in [7] the alloy contained 19.9 at.% Fe). After annealing, we have a  $\text{Fe}_{27.9}\text{Zn}_{72.1}$  compound ( $\Gamma$  phase) which is closer to  $\text{Fe}_8\text{Zn}_{18}$  than to  $\text{Fe}_3\text{Zn}_{10}$ . Two quadrupole doublets with a fixed amplitude ratio of 1 were chosen to fit the MS data points. The two quadrupole doublets Fe<sub>1</sub> and Fe<sub>2</sub> correspond to IT and OH sites respectively. The reason for fixing the amplitude ratio at 1 is that the ratio of the numbers of iron atoms in these two sites is 1. Similarly, for the  $\text{Fe}_3\text{Zn}_{10}$  compound studied in [7] this ratio was 2. The Mössbauer parameters calculated from the fitting of  $\Gamma$  phase are shown in Table 1. As pointed out before, the different MS parameters from [7] obtained from the fitting procedure are probably due to differences in composition.

#### 4. Conclusions

A  $\text{Fe}_{25}\text{Zn}_{75}$  crystalline alloy ( $\Gamma_1$  phase) was formed by mechanically alloying elemental Fe and Zn powders, after milling for 170 h. After an adequate heat treatment, a detailed XRD analysis revealed that the final product is a crystalline alloy of the  $\text{Fe}_{27.9}\text{Zn}_{72.1}$  compound. The unit-cell parameters obtained for these two crystallographic phases, i.e.  $\Gamma_1$  (f.c.c.;  $a = 18.0138 \text{ \AA}$ ) to  $\Gamma$  (b.c.c.;  $a = 8.9936 \text{ \AA}$ ), are in very good agreement with the values in the literature. Further, the results from a DSC measurement allowed us to determine the crystallographic phase transition temperature and its corresponding transition enthalpy. For

the  $\text{Fe}_{25}\text{Zn}_{75}$  phase, whose detailed crystalline structure is still unknown, the MS fitted parameters have allowed us to determine roughly the number of iron atoms in the three different sites in the unit cell.

#### Acknowledgements

We thank J.O. Machado for the XRD measurements and F.G. Mittelstädt for the DSC measurements. One of the authors (E.C. Borba) would like to thank the Conselho Nacional de Desenvolvimento Científico e Tecnológico, Brazil, for financial support.

#### References

- [1] J.M. Poole and J.J. Fischer, *Mater. Technol.*, 9 (1994) 21.
- [2] T. Fukunaga, O. Okasaka, M. Misawa and U. Mizutani, *Kens Rep.*, 9 (1991–1992) 121.
- [3] M. Hansen, *Constitution of Binary Alloys*, McGraw-Hill, New York, p. 737.
- [4] G.F. Bastin, F.J.J. van Loo and G.D. Rieck, *Z. Metallkd.*, 65 (10) (1974) 656.
- [5] A.S. Koster and J.C. Schoone, *Acta Crystallogr., Sect. B*, 37 (1981) 1905.
- [6] J.K. Brandon, R.Y. Brizard, P.C. Chieh, R.K. McMillan and W.B. Pearson, *Acta Crystallogr., Sect. B*, 30 (1974) 1412.
- [7] M.-Y. Gu, G.W. Simmons and A.R. Marder, *Metall. Trans. A*, 21 (1990) 273.
- [8] H.P. Klug and L.E. Alexander, *X-ray Diffraction Procedures*, Wiley, New York, 2nd edn., p. 656.
- [9] B.T. McDermott and C.C. Koch, *Scr. Metall.*, 20 (1986) 669.
- [10] H.M. Rietveld, *J. Appl. Crystallogr.*, 2 (1969) 65.
- [11] A. Johansson, H. Ljung and S. Westman, *Acta Chem. Scand.*, 22 (9) (1968) 2743.